Int. J. Electrochem. Sci., 13 **(2018)** 9346 – 9358, doi: 10.20964/2018.10.61

International Journal of
ELECTROCHEMICAL
SCIENCE
www.electrochemsci.org

Short Communication

Corrosion Characteristics of Aluminum in Highly Diluted Ammonia Solution

Daoyu Li[1], *Yuxi Shi*[2], *Huaping Xu*[1], *Yi Chen*[3], *Pei Zhou*[1], *Xuewu Li*[1], *Wenxin Feng*[1], *Shengping Wang*[2,*]

[1] Guiyang Bureau, Extra High Voltage Power Transmission Company, China Southern Power Grid (CSG), Guiyang 550081, China
[2] Faculty of Material Science and Chemistry, China University of Geosciences, Wuhan 430074, China
[3] Operational Technology Department, Extra High Voltage Power Transmission Company, China Southern Power Grid (CSG), Guangzhou 510663, China
[*]E-mail: spwang@cug.edu.cn

Received: 27 June 2018 / *Accepted:* 8 August 2018 / *Published:* 1 September 2018

Aluminum radiators working with deionized water in high voltage direct current (HVDC) transmission systems were severely corroded. In this paper, the corrosion behavior of aluminum from an aluminum radiator in HVDC in highly diluted ammonia solution was studied, focusing to reduce the corrosion of aluminum in nearly neutral aqueous solution. The surface of the aluminum electrode was covered with $Al(OH)_3$ and/or Al_2O_3, and the corrosion products could reduce further corrosion. It was found that an aluminum electrode in 0.84 μmol L^{-1} ammonia solution had the lowest corrosion rate, and its mechanisms for good corrosion resistance were given. This technology can be used for material anticorrosion in heat-exchange equipment with cooling water.

Keywords: Aluminum, Corrosion, Ammonia solution, Radiator, Thyristor, HVDC

1. INTRODUCTION

High-voltage direct current (HVDC) transmission systems have become the preferred resource allocation and long distance power transportation method for their narrow transmission corridor, high transmission efficiency, and low power consumption [1, 2]. The thyristor in the converter valve, which is a core part of the HVDC system, produces heat while converting alternating current (AC) and direct current (DC) power [3, 4]. The aluminum radiator directly in contact with the thyristor will transfer heat to the cooling water in an inner hole, and heat is transferred by the water in the water cooling circuits. The normal working temperature for a thyristor is approximately 50 °C, which is maintained by the internal water cooling circuits with the aluminum radiator and deionized water. The low conductivity of the cooling water is designed to reduce electrolysis reactions of the water in a strong electric field. In the

internal cooling water cyclic system, in order to increase the resistance of each stream section and minimize the potential differences of the cooling water in each section, several series of platinum grading electrodes will be inserted in the cooling water. However, in the operation process, aluminum hydroxide deposition will occur on the surface of the platinum grading electrodes. As aluminum hydroxide deposition increases on the grading electrodes, the potential differences with the cooling water in each section will also increase. The deposits would drop into the pipe, block the water pipe, reduce the velocity of the flow, and suppress heat transfer.

Covering the surface of aluminum with a layer of aluminum oxide usually stabilizes the surface, making it more difficult to dissolve and corrode [5, 6]. However, if the environment changes, aluminum oxide will still be dissolved, and the internal aluminum will be continuously corroded. The aluminum element in the deposit is formed by corrosion of the aluminum radiator, and aluminum hydroxide is precipitated on the surface of the grading electrodes at appropriate pH values. Therefore, if the corrosion of aluminum could be reduced in the internal cooling water system, the formation of scales on the grading electrode would slow down.

Previous reports covered the corrosion characteristics of aluminum in weak acid medium [7], aqueous alkaline solutions [8, 9] and neutral dilute salt solutions (for instance, halide media [10, 11] and sodium sulfate solution [12]). Different from the above literature, the aim of this paper is to explore the corrosion behavior of aluminum in high purity water with ultralow conductivity. This area of work has not yet been reported in the literature. Reducing the corrosion rate of aluminum in the cooling water with low conductivity at high temperature and retarding the scaling rate of the grading electrode in the valve cooling system are expected. The carbon dioxide pumped into the cooling water system can suppress the scaling of the grading electrode [13], but the corrosion of aluminum was not reduced and the ion adsorption equipment needs to have higher requirements. In this paper, based on the electrochemical corrosion of aluminum at high temperature in an HVDC system, a technique to reduce the corrosion rate of aluminum is discussed. The pH of the cooling water is adjusted using additions of highly diluted ammonia solution to achieve the purpose of inhibiting the corrosion of aluminum.

2. EXPERIMENTAL

2.1. Electrochemical system

An electrochemical system for testing was composed of a working electrode, a reference electrode, a counter electrode and an electrolyte. The working electrodes were cut from the aluminum radiator with a regular shape. The model of the aluminum electrode was 3003 [14], which was composed of Si (0.57 wt%), Fe (0.63 wt%), Cu (0.14 wt%), Mn (1.27 wt%), Zn (0.09 wt%), Li (0.03 wt%) and Al. Apart from the 1 cm ×1 cm working surface, all other surfaces were coated with epoxy resin. Before testing, the working electrodes were degreased, derusted, cleaned with deionized water, dried and immersed in the testing electrolytes for 24 h. Platinum black electrodes were used as counter electrodes, and the reference electrodes were saturated calomel electrodes (SCEs). The potential of SCE at 50 °C is 0.228 V (relative to the standard hydrogen electrode (SHE)). The electrolytes were deionized water and low-concentration ammonia solutions, with concentrations of 0.84, 1.68 and 3.35 μmol L^{-1}. An S470 pH meter was used to test the pH of the electrolytes.

2.2. Electrochemical Test

Steady state polarization curves and electrochemical impedance spectroscopy (EIS) spectra were obtained using the VMP3 electrochemical workstation. The potential scan rate was 1 mV s^{-1}, and the potential range was 0.8 V (ranging from a potential 0.4 V lower than the stable potential to a potential 0.4 V higher than the stable potential). The corrosion potential and corrosion current density were obtained from polarization curves. The corrosion characteristics of the aluminum surface were determined from the results of EIS analysis, which was performed over a frequency range of 10 Hz to 10^5 Hz with an amplitude of 5 mV.

The electrolyte temperatures for all tests were between 48-52 °C. The electrolytic cells were kept in a shielding box during testing.

2.3. Characterization

The electrode surfaces were analyzed by scanning electron microscopy (SEM) and X-ray powder diffraction (XRD) following the steady-state polarization test. The compositions of corrosion products were determined using a D8-Focus X-ray powder diffraction instrument with a Cu target. The scanning angle range was from 5 to 80 degrees, and the scan rate was 8 ° min^{-1}. SEM was done using an SU8010 ultrahigh resolution field emission scanning electron microscope equipped with high performance X-ray energy dispersive spectroscopy (EDS). To study the distribution of the elements in the corrosion products, the microstructure of the aluminum electrode surface was characterized by scanning some areas of the samples with the energy spectrum analyzer.

3. RESULTS AND DISCUSSION

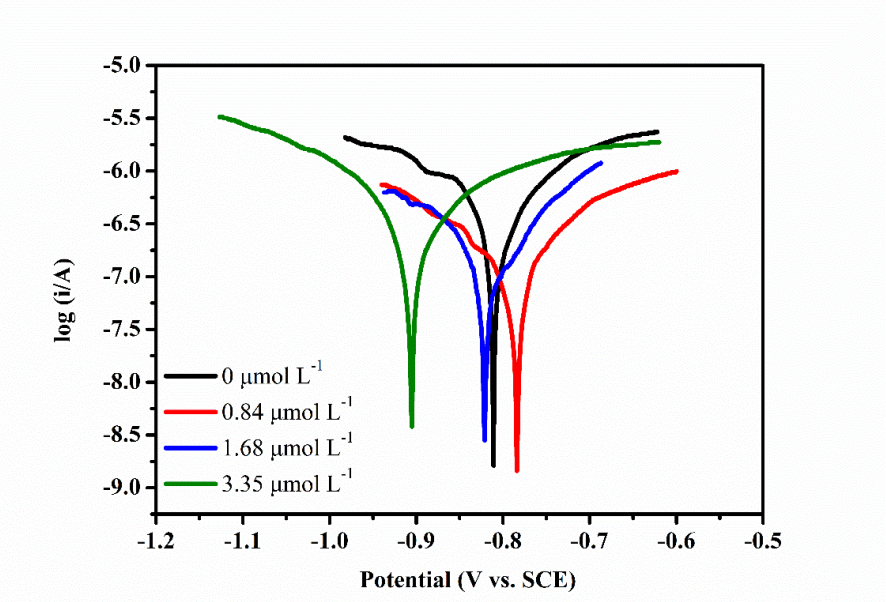

Figure 1. The polarization curves of aluminum in the electrolytes.

The polarization curves of the aluminum electrodes are shown in Fig. 1. The corrosion potential of aluminum in the 0.84 μmol L^{-1} ammonia solution was higher than that in deionized water, thus indicating that the corrosion tendency of aluminum was lower in deionized water. The corrosion potentials of aluminum in the 1.68 and 3.35 μmol L^{-1} ammonia solutions were lower than that in deionized water and 0.84 μmol L^{-1} ammonia solutions. Thus, adjusting the concentration of OH^- in electrolytes by manipulating the ammonia content could reduce the corrosion of aluminum.

The corrosion potential and the corrosion current density of the aluminum electrodes in the electrolytes are shown in Table 1. The lowest corrosion current density and the most positive corrosion potential of aluminum was measured in the 0.84 μmol L^{-1} ammonia solution, indicating that the corrosion rate of aluminum in 0.84 μmol L^{-1} ammonia solution was lowest. The corrosion trend of aluminum in 0.84 μmol L^{-1} ammonia solution was the lowest.

Table 1. Corrosion potentials and corrosion current densities of aluminum in the electrolytes.

Ammonia concentration (μmol L^{-1})	Corrosion potential (V)	Corrosion current density (10^{-7} A cm^{-2})	Anodic Tafel slope (V dec^{-1})	Cathodic Tafel slope (V dec^{-1})
0	-0.811	9.225	0.235	-0.240
0.84	-0.784	1.445	0.262	-0.270
1.68	-0.821	2.818	0.234	-0.347
3.35	-0.905	3.802	0.223	-0.152

The original curve and its corresponding fitting curve of EIS in the electrolytes are shown in Fig. 2. According to the analysis of the surface state of the aluminum electrode, there should be a charge transfer impedance for oxidation of aluminum, a diffusion impedance of ions in the electrolyte, an impedance of the electric double layer capacitor, and an impedance of the cladding layer [15]. R_1 represented the solution resistance between the aluminum electrode and the reference electrode, R_2 represented the impedance of the electrolyte through the deposition layer, R_3 represented the charge transfer impedance for oxidation of aluminum, C_1 represented the capacitance of the cladding layer, C_2 represented the capacitance of the double layer, and W represented the diffusion impedance of ions in the electrolyte [10, 16]. The fitting curves matched the original curve well, which showed that the equivalent circuit diagram can correspond to the basic state of the corrosion reaction of aluminum in the electrolytes.

The corresponding numerical simulation of the equivalent circuit is shown in Table 2. The maximum charge transfer impedance was observed for oxidation of aluminum in 0.84 μmol L^{-1} ammonia solution. This result was consistent with the results of the polarization curves shown in Fig. 1.

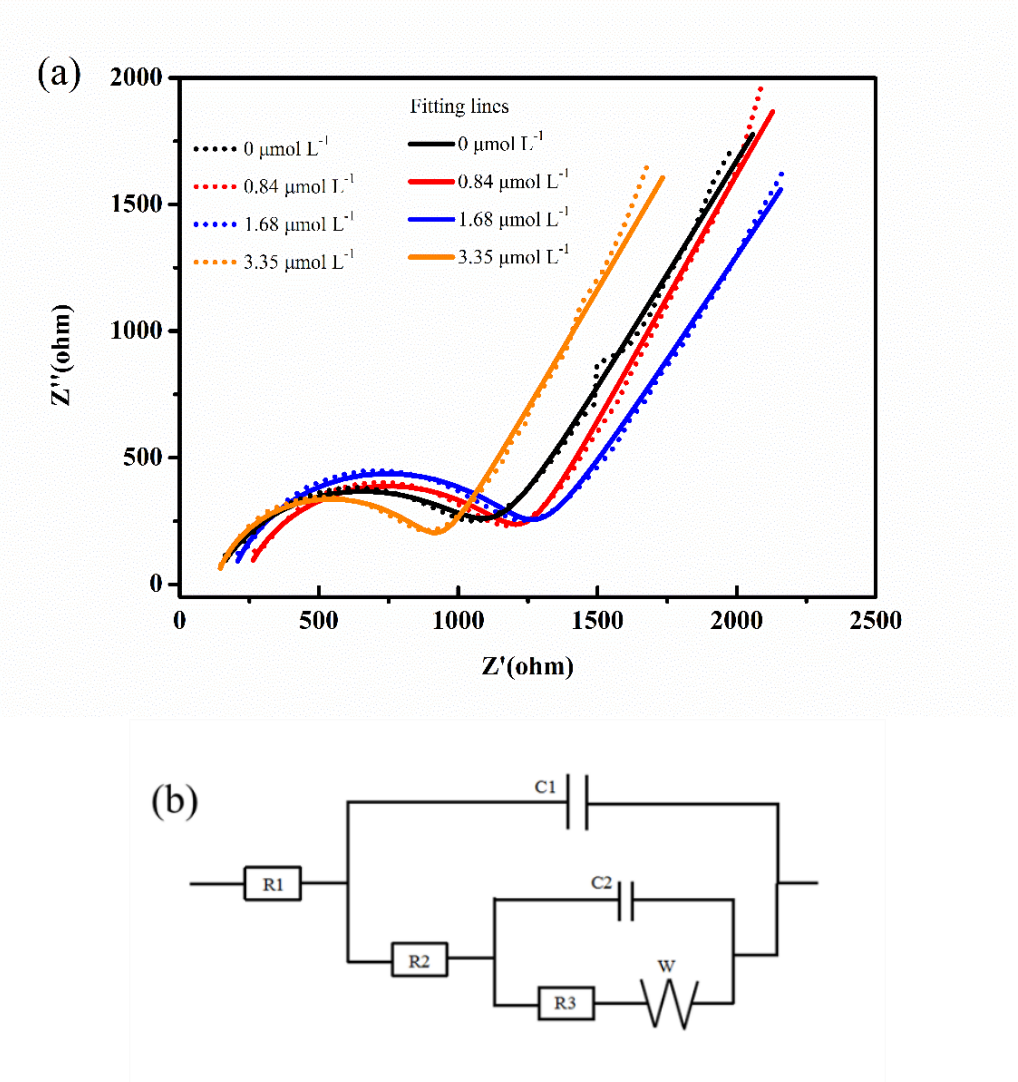

Figure 2. EIS curves (a) and their equivalent circuit diagram (b) for aluminum electrodes in the electrolytes. The original data curves and the fitting curves are indicated by a dotted line and a solid line, respectively.

Table 2. Numerical simulation of EIS.

Concentration (μmol L^{-1})	R_1 (Ω)	R_2 (Ω)	R_3 (10^{-9} Ω)	C_1 (10^{-9} F)	C_2 (10^{-9} F)
0	280.1	867.9	472.6	29.49	1757
0.84	210.1	862.6	701.3	26.04	270.2
1.68	164.8	686.9	512.8	26.15	244.9
3.35	140.3	1095	428.7	10.19	3223

SEM images of the aluminum electrode surface after steady state polarization in the electrolytes are shown in Fig. 3. In deionized water, there was significant corrosion on the aluminum electrode surface; for example, a groove type corrosion trace was observed (Fig. 3a). After corrosion, pits formed on the originally smooth surfaces of the electrodes. The morphology and the corrosion resistance of the aluminum surface were significantly affected (Fig. 3b). The degree of corrosion of the aluminum

electrode in 1.68 and 3.35 μmol L^{-1} ammonia solutions were more serious compared to the degree of corrosion in deionized water (Fig. 3c, d). In Fig. 3e, only the outer layer on the electrode surface showed a small corrosion ditch. The lowest extent of corrosion was observed in the 0.84 μmol L^{-1} ammonia solution, even better compared to corrosion in the deionized water.

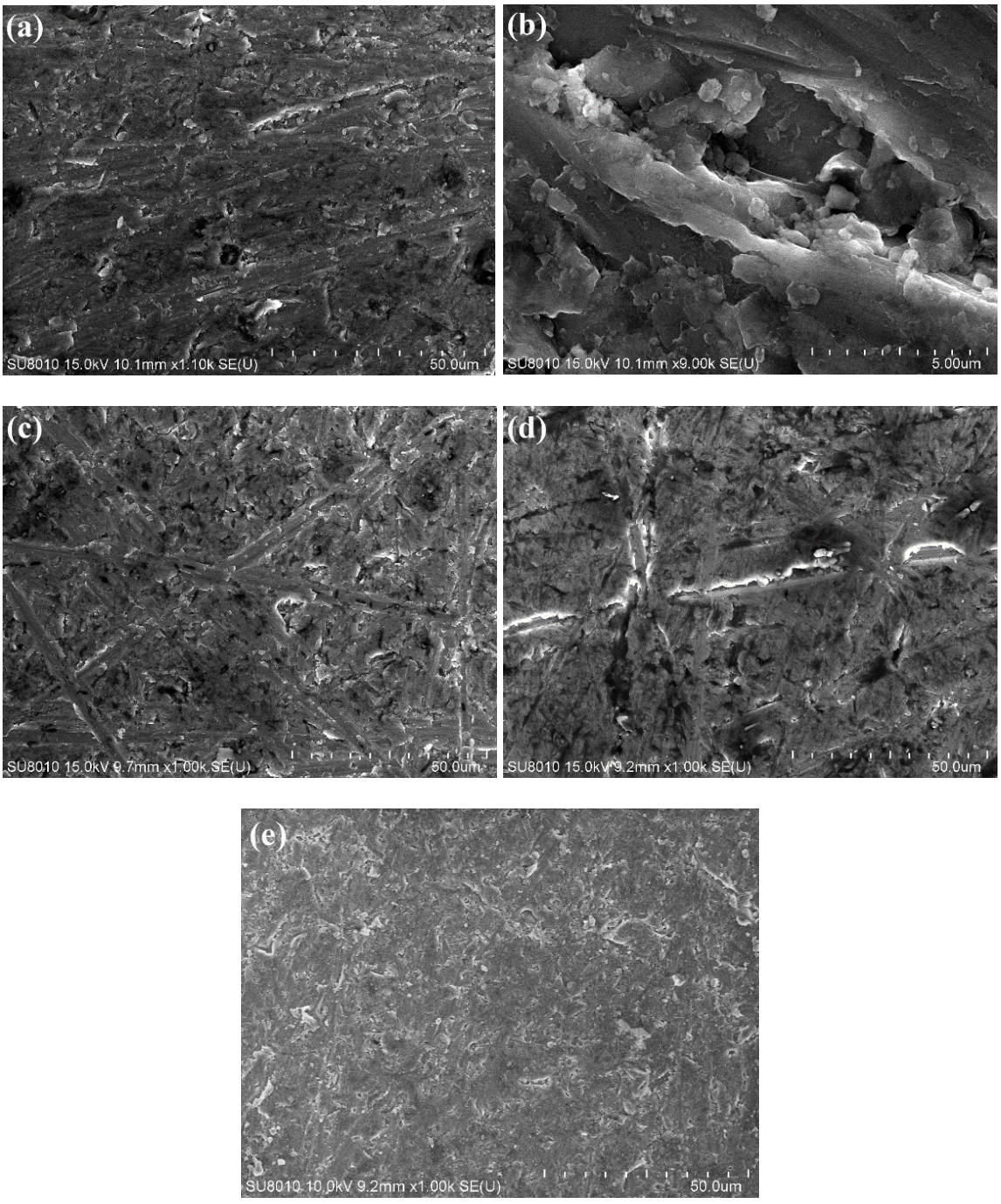

Figure 3. SEM images of the aluminum electrode surface in 0 μmol L^{-1} (a, b), 1.68 μmol L^{-1} (c), 3.35 μmol L^{-1} (d), 0.84 μmol L^{-1} (e) ammonia solution.

The corrosion products of the electrode surface in the 3.35 μmol L^{-1} ammonia solution were tested using EDS. Elemental analysis on the red line region in Fig. 4a gave the types and amounts of the elements of the corrosion products (Fig. 4b), which were mainly aluminum and oxygen. The percentages of the elements are shown in Table 3. The deposits on the electrodes were $Al(OH)_3$ and/or Al_2O_3.

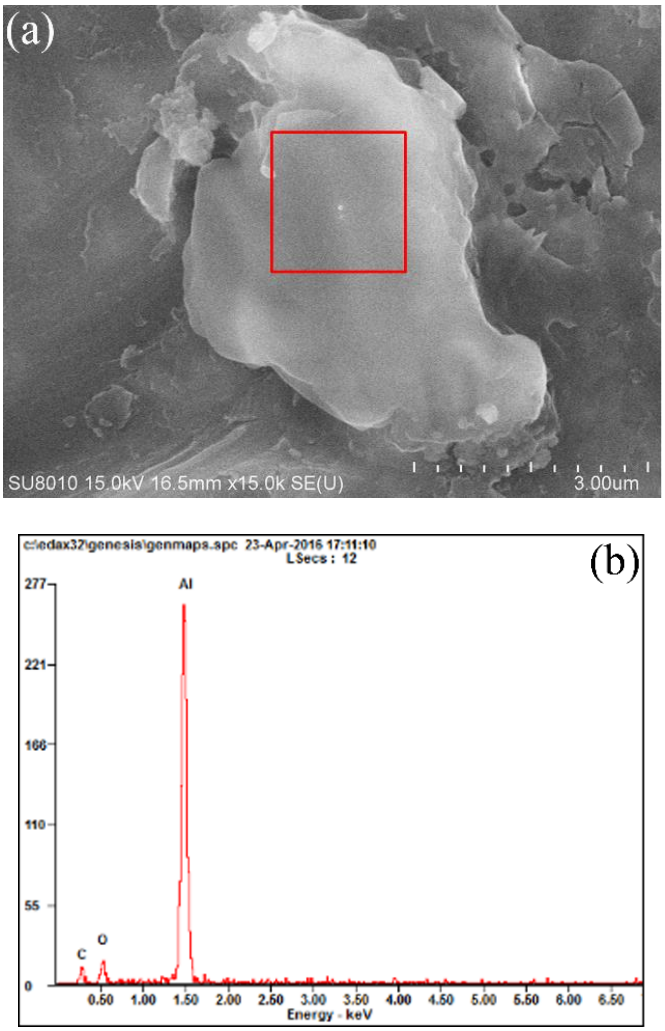

Figure 4. SEM diagram and EDS elemental analysis of corrosion products of aluminum in 3.35 μmol L^{-1} ammonia solution.

Table 3. The content of elements from EDS analysis in Fig. 4.

Element	*Wt%*	*At%*
CK	11.17	21.05
OK	07.74	10.95
AlK	81.09	68.00
Matrix	Correction	ZAF

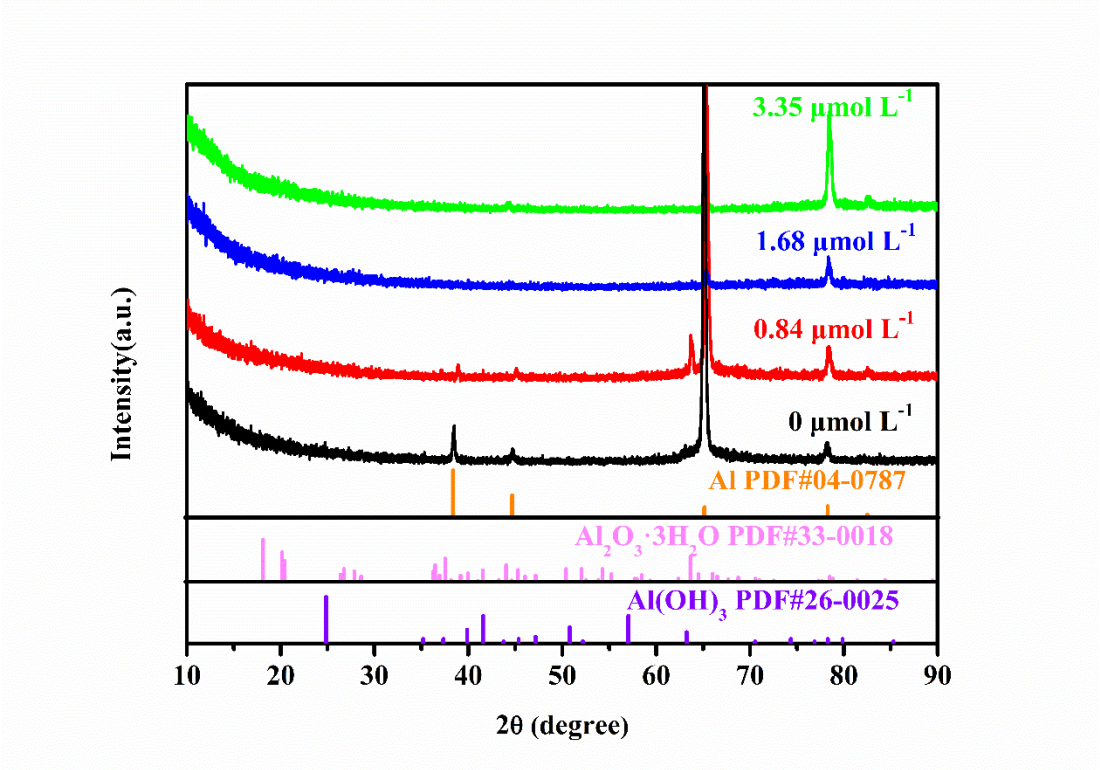

Figure 5. XRD spectrum of corrosion products on the aluminum surface.

XRD spectra of the aluminum electrode surface after steady state polarization tests in the electrolytes are presented in Fig. 5. The corrosion products of all electrodes in the ammonia solutions and the deionized water contained $Al(OH)_3$ (PDF#26-0025). This result was consistent with the results of EDS. Peaks corresponding to $Al_2O_3 \cdot 3H_2O$ (PDF#33-0018) were more prominent in the XRD pattern of the corrosion products when the ammonia concentration was between 0 and 0.84 μmol L^{-1} [17].

These phenomena matched the data from the polarization curves (Fig. 1). The corrosion potential of the aluminum electrode in the 0.84 μmol L^{-1} ammonia solution were more positive, and the corrosion of aluminum was more difficult.

The pH values of the electrolytes were tested and are shown in Table 4. The pH of the deionized water and the low concentration ammonia solutions were near 7.

Table 4. The pH of the electrolyte between 48-52 °C.

Ammonia concentration (μmol L^{-1})	pH
0	5.01
0.84	5.35
1.68	6.99
3.35	7.25

According to the XRD results, the main components of the corrosion products of the aluminum electrode surface were $Al(OH)_3$ and Al_2O_3. This was consistent with the corrosion of aluminum in moist air [16, 18]. Deionized water was used for preparation of the test electrolytes. Some oxygen dissolved in the deionized water when it was exposed to the air. Presumably, the corrosion of aluminum in solution should be a process of dissolution-precipitation [19]. Aluminum first loses some electrons to become Al^{3+}, and then a double electric layer was formed on the electrode surface. Al^{3+} ions combine with OH^- and/or O_2 in the electrolyte to generate $Al(OH)_3$ and/or Al_2O_3 [20, 21]. The precipitation layer covering the electrode surface thickened with continuing corrosion. The corrosion products on the surface prevented further corrosion of the aluminum [22]. However, OH^- can pass through the protective film and contact the inner portion of the aluminum electrode, resulting in the continued corrosion of aluminum.

$$4Al + 3O_2 - 6e^- \rightarrow 2Al_2O_3 \quad (1)$$

In the ammonia solutions, hydrolysis reactions took place, and OH^- ions were generated. The pH of the solution increased.

$$NH_3 \cdot H_2O \rightarrow NH_4^+ + OH^- \quad (2)$$

If the concentration of OH^- was higher, Al_2O_3 and OH^- would combine to generate $Al(OH)_3$ or AlO_2^-.

$$Al_2O_3 + 6OH^- \rightarrow 2Al(OH)_3 + H_2O \quad (3)$$

$$Al_2O_3 + H_2O \rightarrow 2AlO_2^- + 2H^+ \quad (4)$$

Presumably, the corrosion of aluminum in aqueous solution should be a process of dissolution-precipitation. Aluminum first loses some electrons and then attach to the electrode surface in the form of Al_2O_3, which was the initial form of the cladding layer. With further corrosion, partial Al_2O_3 would be transformed into aluminum hydroxide, and the cladding layer thickened. However, ions (OH^- or Al^{3+}) could pass through the cladding layer and react with the inner aluminum layer, resulting in continued corrosion of the aluminum. The cladding layer could prevent further corrosion of the aluminum.

The corrosion potential in 0.84 μmol L^{-1} ammonia solution was higher than corrosion potentials in 1.68 and 3.35 μmol L^{-1} ammonia solutions and in the deionized water. Referring to the pH of the electrolyte and electrode potential of the aluminum electrode, the Pourbaix diagram of aluminum-water at 25 °C was divided into a corrosion zone, passivation zone and corrosion-free zone. Aluminum would not corrode easily in the passivation area. Thus, the corrosion rate and corrosion trend in the passivation area were low. When the concentration of soluble ions in the solution was 10^{-6} mol L^{-1}, the impedance of the corresponding corrosion reaction was relatively large, and corrosion could not take place. The Pourbaix diagram of aluminum-water between 48 and 52 °C was similar to that at 25 °C, which still possessed guiding significance for the corrosion prediction of aluminum [23].

The corrosion reaction of aluminum at 50 °C (323.15 K) could be divided into 2 cases. Their corresponding thermodynamic data were calculated. The basic thermodynamic data for calculation are listed in Table 5 [24]. Additionally, R=8.314 J mol^{-1} K^{-1} and F=96500 C mol^{-1}.

Table 5. Some thermodynamic parameters.

	298.15 K, 100 kPa		
	$\Delta_f G_m^\theta$ （kJ mol^{-1}）	$\Delta_f H_m^\theta$ （kJ mol^{-1}）	S_m （J mol^{-1} K^{-1}）
H_2O（l）	-237.14	-285.830(40)	69.95(3)
H^+ (aq)	0	0	0
OH^-	-157.28	-230.015	-10.90
Al^{3+}	-485.3	-538.4	-325.(10)
AlO^{2-} (aq)	-830.9	-930.9	-36.8
Al_2O_3 (corundum)	-1582.3	-1675.7(13)	50.92(10)
Al	0	0	28.30(10)
$Al(OH)_3$	-1306	-1284	71

In the 1st case, aluminum corrosion generated Al^{3+} at lower pH. When the concentration of Al^{3+} in solution was 10^{-6} mol L^{-1}, the aluminum turned to the corrosion free zone or passivation zone.

$$Al \rightarrow Al^{3+} + 3e^- \quad (5)$$

$$E(Al^{3+}/Al) = E^{\theta}(Al^{3+}/Al) - \frac{0.0592}{3}\log\left(\frac{1}{C(Al^{3+})}\right) \quad (6)$$

$$E(Al^{3+}/Al) = -1.470 + 0.0197\log\left(C(Al^{3+})\right) \quad (7)$$

When $C(Al^{3+})$ was 10^{-6} mol L^{-1}, $E(Al^{3+}/Al)$ was -1.588 V.

In the 2nd case, aluminum corrosion generated AlO_2^- at higher pH. Similarly, when the concentration of AlO_2^- in the solution is 10^{-6} mol L^{-1}, aluminum also turned to the corrosion free zone or the passivation zone.

$$Al + 2H_2O \rightarrow AlO_2^- + 4H^+ + 3e^- \quad (8)$$

$$E(AlO_2^-/Al) = E^{\theta}(AlO_2^-/Al) - \frac{0.0592}{3}\log\left(\frac{1}{C^4(H^+)C(AlO_2^-)}\right) \quad (9)$$

$$E(AlO_2^-/Al) = -1.01 + 0.0197\log\left(C(AlO_2^-)\right) - 0.0789pH \quad (10)$$

$$E(AlO_2^-/Al) = -1.1282 - 0.0789pH \quad (11)$$

When pH was 7, the electrode potential was -1.681 V.

In an aqueous solution, Al^{3+} and AlO_2^- react with each other with changing pH, resulting in the following reactions:

$$Al^{3+} + 2H_2O \rightarrow AlO_2^- + 4H^+ \quad (12)$$

$$K^{\theta} = \frac{C(AlO_2^-)C^4(H^+)}{C(Al^{3+})} \quad (13)$$

$$\Delta_r G_m^{\theta} = -RT\ln K^{\theta} = -RT\ln\frac{C(AlO_2^-)}{C(Al^{3+})} - 4RT\ln C(H^+) \quad (14)$$

$$\log\frac{C(Al^{3+})}{C(AlO_2^-)} = -\log K^{\theta} - 4pH \quad (15)$$

$$\log\frac{C(\mathrm{Al^{3+}})}{C(\mathrm{AlO_2^-})} = 21.42 - 4\mathrm{pH} \quad (16)$$

When the concentration of Al^{3+} and AlO_2^- in solution were equal to each other or were both lower than 10^{-6} mol L^{-1}, the pH was 5.35.

At 50 °C, when the potential of aluminum is higher than -1.588 V (vs. SHE) with low pH or -1.681 V (vs. SHE) with high pH, aluminum in a certain range of pH was in the passivating zone with a lower extent of corrosion. When the pH of the solution was below or above the range mentioned, aluminum corrosion easily occurred. According to Eq. 16, when the pH was 5.35, the concentration of Al^{3+} in the electrolyte equaled to that of AlO_2^-, and the concentration of Al^{3+} (or AlO_2^-) in the solution was at its lowest. The corrosion resistance of aluminum was quite high, and the corrosion trend was the weakest [18].

At 50 °C, the following reaction would take place in an aqueous solution. According to XRD results, the main product on the surface of the aluminum electrode was aluminum hydroxide. Thus, the subsequent discussions will be based on aluminum hydroxide.

$$\mathrm{Al^{3+} + 3H_2O \rightarrow Al(OH)_3 + 3H^+} \quad (17)$$

$$K^\theta = \frac{C^3(\mathrm{H^+})}{C(\mathrm{Al^{3+}})} \quad (18)$$

$$\log\left(K^\theta\right) = -\log\left(C(\mathrm{Al^{3+}})\right) - 3\mathrm{pH} \quad (19)$$

$$\log\left(C(\mathrm{Al^{3+}})\right) = 9.08 - 3\mathrm{pH} \quad (20)$$

When $C(Al^{3+})$ was 10^{-6} mol L^{-1}, the pH was 5.03.

$$\mathrm{Al(OH)_3 \rightarrow AlO_2^- + H_2O + H^+} \quad (21)$$

$$K^\theta = C(\mathrm{H^+})C(\mathrm{AlO_2^-}) \quad (22)$$

$$\log\left(K^\theta\right) = \log\left(C(\mathrm{AlO_2^-})\right) - \mathrm{pH} \quad (23)$$

$$\log\left(C(\mathrm{AlO_2^-})\right) = -12.87 + \mathrm{pH} \quad (24)$$

When $C(AlO_2^-)$was 10^{-6} mol L^{-1}, the pH equaled to 6.87.

According to Eqs. 17-24, at pH<5.3, the slope of the $\log\left(C(\mathrm{Al^{3+}})\right)$-pH curve was -3. When pH>6.87, the slope of the $\log\left(C(\mathrm{AlO_2^-})\right)$-pH curve equals to 1. The corrosion of aluminum was more sensitive to pH at low pH values. The smaller differences between the practical pH and the lowest corrosion pH lead to increased corrosion.

According to Eq. 16, at a pH value of 5.35, the concentration of Al^{3+} (or AlO_2^-) in the electrolyte was at its lowest. The pH of 0.84 μmol L^{-1} ammonia was exactly 5.35; the corrosion resistance was at its highest and the corrosion trend was the weakest in this case. The pH of deionized water was 5.01. According to Eq. 20, the concentration of Al^{3+} was $10^{-5.959}$ mol L^{-1}. The pH of ammonia with concentrations of 1.68 and 3.35 μmol L^{-1} were 6.99 and 7.25, respectively. According to Eq. 24, the concentrations of AlO_2^- for these solutions were $10^{-5.883}$ and $10^{-5.619}$ mol L^{-1}, respectively. According to thermodynamic analysis, in the 0.84 μmol L^{-1} ammonia solution, the concentrations of soluble components were at their lowest and the corrosion rate of aluminum was at its slowest.

Al^{3+} (or AlO_2^-) in the circulating cooling water in the HVDC system was continuously removed after going through the ion adsorption equipment. As a result, the concentration of Al^{3+} (or AlO_2^-) in the cooling water has not been maintained. The passivation state of aluminum was difficult to maintain, and aluminum was continuously corroded into the solution. The pH of the 0.84 μmol L^{-1} ammonia solution

contributed to the weakest corrosion of aluminum, so the corrosion rate of aluminum was the lowest under this condition.

4. CONCLUSIONS

The corrosion behavior of aluminum in neutral aqueous solution was proposed. The aim is to reduce the corrosion of aluminum radiators and the scaling of grading electrodes in HVDC with special requirements, such as the ultralow conductivity of the cooling water. In electrolytes with pH near 7, the OH^- concentration on the aluminum surface would affect the corrosion trend of aluminum. At 50 °C, the corrosion of aluminum in 0.84 μmol L^{-1} ammonia solution was lower than in deionized water, and lower than in an ammonia solution with higher concentration. This behavior will have great significance for the application of aluminum in HVDC.

ACKNOWLEDGMENTS
This work was supported by the Programs of the China Southern Power Grid (CGYKJXM20160094).

References

1. A. Kalair, N. Abas and N. Khan, *Renew. Sust. Energ. Rev.*, *5*9 (2016) 1653.
2. B.V. Eeckhout, D.V. Hertem, M. Reza, K. Srivastava and R. Belmans, *Euro. Trans. Electr. Power*, 20 (2010) 661.
5. M. Barnes and A. Beddard, *Energy Procedia*, 24 (2012) 108.
6. A. Korompili, Q. Wu and H. Zhao, *Renew. Sust. Energ. Rev.*, 59 (2016) 1405.
7. C.H. Liang, K. Liang and N.B. Huang, *Mater. Sci. Tech.*, 19 (2011) 52.
8. J.P. Dasquet, D. Caillard, E. Conforto, J.P. Bonino and R. Bes, *Thin Solid Films*, 371 (2000) 183.
9. I.V. Aoki, M.C. Bernard, S.I.C. Torresi, C. Deslouis, H.G. de Melo, S. Joirt and B. Tribollet, *Electrochim. Acta*, 46 (2002) 1871.
10. J. Wysocka, S. Krakowiak, J. Ryl and K. Darowicki, *J. Electroanal. Chem.*, 2016, 778 (2016) 126.
11. J.B. Wang, J.M. Wang, H.B. Shao, J.Q. Zhang and C.N. Cao, *J. Appl. Electrochem.*, 37 (2007) 753.
12. B. Zhang, Y. Li and F. Wang, *Corros. Sci.*, 51 (2009) 268.
13. M. Lashgari, E. Kianpour and E. Mohammadi, *J. Mater. Eng. Perform.*, 22 (2013) 3620.
14. A. Viomar, M. Terada, I. Costa I, P.R.P. Rodrigues, C. Schlindwein and E.P. Banczek, *Matéria*, 20 (2015) 420.
15. I. Weber, B. Mallick, M. Schild, S. Kareth, R. Puchta and E.R. Van, *Chem. Eur. J.*, 20 (2014) 12091.
16. BSI, BS ISO 209-2007.
17. M. Trueba and S.P. Trasatti, *Corros. Rev.*, 33 (2015) 373.
18. W. C. Moshier, G.D. Davis and J.S. Ahearn, *Corros. Sci.*, 27 (1987) 785.
19. B. Li and L. L. Shao, *Inorg. Chem. Indu.*, 40 (2008) 54
20. E. Deltombe and M. Pourbaix, *Corros.*, 14 (1958) 16.
21. H.S. Lee, J.K. Singh and J.H. Park, *Constr. Build. Mater.*, 113 (2016) 905.
22. Z. Szklarska-Smialowska, *Corros. Sci.*, 41 (1999) 1743.
23. S. He, H. Ye, Y. Ma, L. Guo, Y. Gou and P. Zhang, *Corros. Sci.*, 107 (2016) 21.
24. A. Pardo, M.C. Merino, A.E. Coy, R. Arrabal, F. Viejo and E. Matykina, *Corros. Sci.*, 50 (2008) 823.
25. C.Y. Liang and K. Wang, *Chem. Bull.*, 5 (1977) 44.

26. J.G. Speight, Lange's Handbooks of Chemistry, 16th, McGraw-Hill, (2005), Laramie, Wyoming, USA, 1.15 Table 1.56.